Egypt. J. Chem. **Vol. 67**, No. 7 pp. 127 - 139 (2024)

Egyptian Journal of Chemistry

http://ejchem.journals.ekb.eg/

Tinuvin-P Metal Complexes as New Photo-Stabilizers for PVC: Synthesis, Characterization and DFT Studies

Mohamed A. El Awady[1], Mostafa M.H. Khalil[1,*], Gehad G, Mohamed[2,3], Abdel Naby M. Salem[1]

[1]*Chemistry Department, Faculty of Science, Ain Shams University, Abbassia, 11566, Cairo, Egypt*
[2]*Chemistry Department, Faculty of Science, Cairo University, Gamaa Street, Giza 12613, Egypt*
[3]*Nanoscience Department, Basic and Applied Sciences Institute, Egypt-Japan University of Science and Technology, New Borg El Arab, Alexandria, 21934, Egypt*

Abstract

In the present study, new metal complexes of Tinuvin-P (Tp), a well-known photostabilizer for vinyl polymers, $[Co(Tp)_2(H_2O)_2]$ 0.5EtOH (**1**), $[Ni(Tp)_2(H_2O)_2]$ $1.5H_2O$(**2**), $[Cu(Tp)_2(H_2O)_2]$EtOH(**3**) and $[Zn(Tp)_2]H_2O$ (**4**) have been synthesized, characterized (elemental analyses, FT-IR, ^{1}H-NMR, UV-vis., MS, EPR, magnetic, TG and conductivity), and investigated as photo-stabilizers for PVC. Theoretical calculations involving geometry optimization have been performed at the DFT/B3LYP level of theory. According to the spectral data, Tp behaved as a mononegative bidentate ligand and coordinated with metal ions via deprotonated phenolic O and triazole N. According to Uv-vis, EPR, and magnetic moment measurements, complexes **1-3** have octahedral geometry, while complex **4** has tetrahedral geometry. XRD study pointed out that complex 1 is amorphous while complexes 2-4 were semicrystalline. The photostabilization efficiency results, based on the determination of percent weight loss and the percent gelation, showed a rational stabilizing effect of the studied complexes compared with the free ligand, and the stabilizing efficiency was found to be in the following order: ***1>2>Tp>4 ~ 3***. The optimized structures of the ligand and its investigated complexes as the lowest energy configurations were carried out at B3LYP/6-311G (d, p) level at the density functionaltheory (DFT) level. The Co (II)-complex (**1**), with the lower ionization potential, higher dipole moment, and lowest E_g, was found to be highly effective as a light stabilizer agent than the ligand and other complexes.

Keywords: Photo-stabilizer; Tinuvin P; PVC; NBO; Metal complexes

1. Introduction

Polyvinyl chloride (PVC) is a synthetic plastic polymer that ranks second in terms of production volume after polyethylene. It finds extensive usage in various industries, including architecture, electronics, chemical engineering, packaging, and transportation [1]. The low-cost and superior performance of PVC have led to its increased adoption in the construction sector, particularly for exterior applications such as siding, cladding, and window profiles [2]. However, the capacity of the PVC materials to resist photo-degradation causes hydrogen chloride loss, discoloration, and severe corrosion phenomena, along with modifications to its chemical and physical properties during prolonged light exposure [3, 4]. As a result, precautions should be taken during the production of plastic to ensure that the materials survive longer and to prevent photooxidation and photodegradation processes. UV absorbers are crucial in the process of absorption of damaging ultraviolet

*Corresponding author e-mail:khalil62@yahoo.com.; (Mostafa M.H. Khalil).
EJCHEM use only: Received date 30 November 2023; revised date 31 December 2023; accepted date 03 January 2024
DOI: 10.21608/EJCHEM.2024.250821.8921

radiation and dispersing it as safe thermal energy. They prevent the development of free radicals, which are created during the initial phases of deterioration. Recently, the most popular additives utilized for study are organic Schiff bases [5] and organometallic complexes [6,7], but the most popular industrial UV absorbers are carbon black, titanium dioxide, benzophenones, and triazoles (such as hydroxybenzophenone). Additionally, coordination complexes of Ni(II), Cu(II), Zn(II), Cd(II), and Sn(II) metals with [4-amino-5-(pyridyl)-4H-1,2,4-triazole-3-thiol] have been synthesized and employed as photostabilizers for polystyrene [8].

So far, 2-(2ˈ-hydroxy-5ˈ-methylphenyl) benzotriazole (Tinuvin-P, Tp) [9] was investigated as ultraviolet-light absorbers (UVAs) for some polymeric materials, paints, cosmetics, and contact lenses [10]. Stabilizers were used to protect plastic compounds against the effect of UV light and hence act to prevent oxidation from that source [11]. Addition of UVA to the polymeric materials slows their photo-oxidation both by absorbing UV and by quenching the excited species that might initiate free radical oxidation [12]. Tp has several advantages over other photostabilizers such as strong absorption of UV radiation, high UV absorption efficiency, excellent resistance to the oxidizing and reducing agents used as additives in the curing, and polymerization, and synergistic performance with the other stabilizers. Conversely, it bears the disadvantages of high volatility at high processing temperatures and needs a substantial thickness to work effectively hence is not really suitablefor very thin products, textiles, or films. Since the discovery of Tp as a UVA, most efforts have been focused on studying the effect of different substituents in the benzotriazole moiety [13] more than in the variation of using different heterocyclic rings. Metal complexes of Tp and its derivatives [14, 15] are also the subject of intensive research owing to their rich coordination chemistry and the importance of the benzotriazole moiety, which can adopt a variety of coordination modes to give mono and polynuclear complexes [15]. [Zn(Tp)(CH3COO)(H2O)2] and [Zn(Tp)2(H2O)2] complexes have been prepared by Mostafa et al., [14] assuming that Tp interacted with Zn(II) ions as a mono-negatively bidentate ligand.

The photostabilization of PVC films using 4-(benzylideneamino)-5-(pyridin-4-yl)-4H-1,2,4-triazole-3-thiol metal complexes (M = Ni (II), Cu(II), Zn(II), Sn(II) and Cd(II)) was studied [16]. The additives were found to possibly act as HCl scavengers, UV absorbers, and peroxide decomposers which ultimately contribute to the stabilization of PVC films. Among the Schiff's base metal complexes tested, the Ni(II) complex exhibited the highest efficiency in photostabilizing PVC.

In the present study, Co(II), Ni(II), Cu(II), and Zn(II) complexes of Tp have been synthesized, characterized, and investigated for the stabilization of the rigid PVC against the photo-degradation aiming to enhance the efficiency of Tp as a photo-stabilizer. Quantum chemical calculations of the optimized molecular geometries and electronic populations in terms of natural bond orbital analysis (NBO) [17] have been examined. NBO analysis was also used to identify the nature of the interaction between ligand and central metal ion.

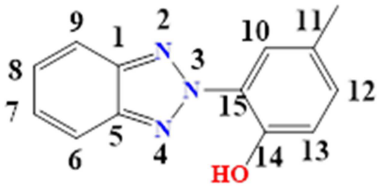

Tinuvin-P, Tp

2. Experimental

2.1. Synthesis

One mmol hot ethanolic solution of Tp (225 mg, 20 ml) was mixed with one mmol aqueous solution (7 ml) of $Co(NO_3)_2 \cdot 6H_2O$ (291 mg), $NiCl_2 \cdot 6H_2O$ (238 mg), $Cu(NO_3)_2 \cdot 3H_2O$ (241 mg) or $ZnCl_2 \cdot 4H_2O$ (136 mg). The resulting mixtures were heated to reflux, whereupon the complexes were precipitated. The low molar conductivity values (7.00-25.20 Ω-1cm2mol-1) of the studied complexes (in DMF) reflect their non-electrolytic nature [18]. Single crystals could not be obtained, as the complexes only form amorphous materials as shown by their XRD patterns.

-**Tp** ($C_{13}H_{11}N_3O$)**:**Color: Slightly yellow. FT-IR (cm^{-1}): 3396ν(O-H), 1595 ν(C=N) + ν(C=C), 1063 ν(N-N). ^{1}H-NMR (DMSO-d_6, δ, ppm): 10.35 (s,1H, H17), 8.05 (d,1H, H9), 8.05 (d, 1H, H6), 8.03 (t, 1H, H7), 7.68 (s, 1H, H15), 7.55 (t, 1H, H8), 7.22 (d, 1H, H13), 7.08 (d, 1H, H12), 2.32 (s,

3H, H16). UV-Vis. (C_2H_5OH, 5×10^{-5}, nm): 210, 239, 297, and 337 nm.

- **Complex (1) ($C_{26}H_{24}CoN_6O_4.0.5EtOH$):** Color: Reddish yellow. Yield: 62.5%.Elemental analysis (%): Calcd. C 56.14, H 4.76, N 14.82, found: C 56.50, H 4.73, N 14.53 FT-IR (cm^{-1}): 3405 ν(OH), 1615 ν(C=N), 943 ν(N-N), 435 ν(Co-N), 492 ν(Co-O). UV-Vis. (DMF, 10^{-4}, nm): 292, 339, and 770, Molar Cond.. (10^{-3} M, DMF, $\Omega^{-1}cm^2mol^{-1}$): 25.20. μ_{eff} (μ_B, 298 K): 4.29 μ_B.
- **Complex (2)** ($C_{26}H_{24}NiN_6O_4.1.5H_2O$):Color: Greenish yellow. Yield: 80%.Elemental analysis (%): Calcd. C 54.76, H 4.73, N 13.70, found: C 54.08, H 4.44, N 14.33.FT-IR (cm^{-1}): 3421 ν(OH), 1615 ν(C=N), 1498 ν(C=C),1560, 982 ν(N-N), 432 ν(Ni-N), 495 ν(Ni-O). UV-Vis. (DMF, 10^{-4}, nm): 299, 339, and 645. Molar Cond. (10^{-3} M, DMF, $\Omega^{-1}cm^2mol^{-1}$): 14.70. μ_{eff} (μ_B, 298 K): 4.63 μ_B.
- **Complex(3)** ($C_{26}H_{24}CuN_6O_4.EtOH$):Color: Reddish yellow. Yield: 53.3%.Elemental analysis (%): Calcd. C 56.41, H 5.03, N 14.10, found: C 56.50, H 4.88, N 14.18. FT-IR (cm^{-1}): 3432 ν(OH), 1615 ν(C=N), ν(CO)1252, 985 ν(N-N), 435 ν(Cu-N), 493 ν(Cu-O). UV-Vis. (DMF, 10^{-4}, nm): 298, 335, and 840. Molar Cond. (10^{-3} M, DMF, $\Omega^{-1}cm^2mol^{-1}$): 7.0. μ_{eff} (μ_B, 298 K): 2.13 μ_B.
- **Complex(4)** ($C_{26}H_{20}ZnN_6O_2.H_2O$):Color; Pale yellow. Yield: 75%.Elemental analysis (%):Calcd. C 58.49, H 4.12, N 15.74, found: C 58.00, H 4.17, N 15.38. FT-IR (cm^{-1}): 3090 ν(OH), 1613 ν(C=N), 1498 ν(C=C), 943 ν(N-N), 437 ν(Zn-N), 497 ν(Zn-O). ^{1}H-NMR (DMSO-d_6, δ, ppm): 10.32 (s, 1H, H17), 8.05 (d, 1H, H6), 8.03 (t, 1H, H7), 7.99 (t, 1H, H8), 7.69 (d, 1H, H9), 7.54 (s, 1H, H15), 7. 24 (d, 1H, H13), 7.12 (d, 1H, H12), 2.31 (s, 3H, H16). UV-Vis. (DMF, 10^{-4}, nm): 297, 337. Molar Cond. (10^{-3} M, DMF, $\Omega^{-1}cm^2mol^{-1}$): 9.30.

2.2. Physical measurements

FT-IR spectra were measured as KBr pellets using a Jasco FTIR 460 plus. The UV/Vis spectra were scanned on a Shimadzu UV-2600 solid-state UV–vis spectrophotometer. The mass spectra were recorded with the aid of a Shimadzu QP-2010 plus mass spectrometer at 70 eV.^{1}H-NMR spectra were run at 300 MHz in DMSO-d_6 using Varian-Oxford MercuryVX-300 NMR. The Shimadzu DTG-60H simultaneous DTG/TG apparatus was utilized to conduct TGA in a platinum crucible with a heating rate of 10 ºC min-1, under N_2 atmosphere (20 ml min-1) Magnetic measurements were carried out on a Sherwood scientific magnetic balance using Gouy method [19], and $Hg[Co(SCN)_4]$ as a calibrant. Elemental analyses were performed using Elemental Vario EL III. A digital Jenway 4310 conductivity meter (cell constant 1.02) was used for the determination of the molar conductance. X-ray powder diffraction was performed using Philips X-ray diffractometer model PW 1840 with copper anode (K_α, λ = 1.54056 Å) operated at 40 kV and 25 mA.X-band EPR measurements were performed on solid samples at 298 K using a Bruker EMX spectrometer. The *g*-values were obtained by referencing to a diphenylpicrylhyrdazyl (DPPH) sample with g = 2.0036. The modulation amplitude was suited at 4 Gauss while the microwave frequency was determined as 9.775 GHz.

2.3. DFT calculations

The Gaussian 09 program package was utilized to conduct DFT calculations on both the ligand and its metal complexes [20]. The Gauss View 5.0 package was employed to examine different graphical representations of molecular charges and the shapes of molecular orbitals.

2.4. Preparation of PVC polymeric film samples

Homogenous films of PVC (additive free, and K = 70, supplied by Hüls company-Germany) were prepared by dissolving 0.75 g of PVC in THF, where the investigated complexes and the reference stabilizer (2% wt) were added to the PVC solution. After obtaining the solutions, they were poured into a Petri dish that had a constant diameter and leftovernight at room temperature until the complete evaporation of THF [21]. The films were 20-30µm thick in all cases.

2.5. Photo-degradation experiments

The photodegradation process was achieved using a 375WPRK-2M type UV lamp covering the full range of the UV region, where the examined samples were held at a constant distance of 15 cm. The temperature across the sample was kept constant at 70±2 ºC [22]. The stabilizing efficiency of the compounds under investigation was evaluated

through weight loss and gel formation. The first approach involved measuring the percentage of weight loss resulting from the irradiation process, which was calculated using the equation:

$$\text{Weight loss } (\%) = [(W_1 - W_2)/W_1] \times 100 \quad (1)$$

Where: W_1 and W_2 are the weight of the sample before and after the irradiation process, respectively.

The second method involved determining the gel content by dissolving constant weights (0.5 g) of each sample in 20 ml THF at 35 ºC overnight, followed by photolysis for various time intervals. The insoluble fractions were separated by centrifugation, washed with the solvent, and dried to constant weight in the oven. The % gel was calculated using the formula:

$$(\%)\ \text{Gel} = (W_2/W_1) \times 100 \quad (2)$$

Where W_1 is the weight of the original sample and W_2 is the weight of the insoluble fraction (gel fraction).

Additionally, the soluble fractions were precipitated in cold methanol, filtered, and dried in an air-oven to constant weight. The percentage of the soluble fractions was then determined to ensure the accuracy of the previously determined gel amount.

$$(\%)\ \text{Soluble fraction} = (W_2/W_1) \times 100 \quad (3)$$

Where: W_1 is the weight of the original sample and W_2 is the weight of the soluble fraction after precipitation in methanol (after complete evaporation of the solvent and complete dryness).

3. Results and discussion

3.1. IR

The IR spectrum of Tp showed a broad band at 3396 cm^{-1} assigned to ν(OH). This mode disappears in complexes supporting that this group is involved in the complex formation with loss of the proton [23]. However, the presence of weak bands in the range 3450-3375 cm^{-1} in the complexes is due to the presence of EtOH and H_2O in the complexes. The assignment of ν(C=N) mode alone is difficult owing to the involvement of C=N in intra-molecular H-bond with the phenolic group [15]. Coordination of Tp to the metal ion *via* the benzotriazole ring resulted in the appearance of ν(C=N) mode at lower wave numbers, 1615 **(1, 2 3),** and 1613 cm^{-1}**(4)**. Besides, the ν(N-N) mode observed at 1063 cm^{-1} in Tp is found at lower wave numbers in the complexes, 943-982 cm^{-1}, confirming the participation of the benzotriazole in chelation [24].Moreover, the complexes exhibited new non-ligand bands in the range of 601-563 cm^{-1} and the range of 452-428 cm^{-1} assigned to M-N and M-O bond formation in the complexes.

3.2. ^{1}H-NMR

The ^{1}H-NMR spectrum of free Tp exhibited a singlet signal at δ 10.35 ppm in DMSO-d_6 assigned to the phenolic OH involved in an intramolecular hydrogen bond. This signal is missed in Zn(II) complex **4** suggesting that the OH group participates in the complexes, through the replacement of the hydroxy proton by the metal ions (Figure 1).

The signals of the benzotriazole protons are shown at 7.55 and 8.04 ppm corresponding to two triplets (H7 and H8) and two doublets (H6 and H9) signals, respectively, while the signals of the phenolic moiety appear as singlet and two doublets at 7.09 (H15), 7.22 (H12) and 7.66 (H13) ppm [25]. The signal of the methyl group appears as a singlet at 2.31 ppm. For complex **4**, the aromatic protons nearest the coordination centers are found to suffer maximum downfield shifts compared with the other aromatic protons.

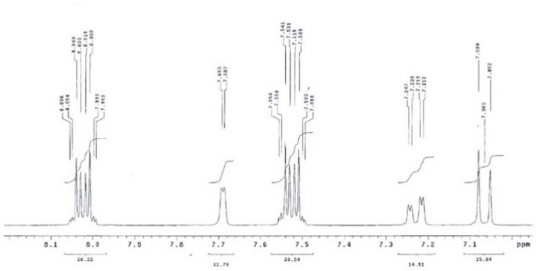

Figure 1: ^{1}H-NMR spectrum of Zn(II)-Tp complex in DMSO

3.3. TGA

The thermal stability and degradation behavior of some of the reported complexes were studied using the thermogravimetric (TG) technique. Thermal decomposition of complex **1** occurs through two endothermic steps maximized at 221 and 422 ^oC. The 1st step (50-300 ^oC) may be thought to be due to the desorption of 0.5 H-bonded ethanol, 2 H_2O molecules and one Tp molecule with a mass loss amount to 49.42% (calcd. 50.00%). The 2nd step occurring within the 300-1000 ^oC range is allocated to the loss of another Tp molecule, leaving Co as the

final residue (observed overall mass loss, 93.57%, calcd. 89.62%). Complex **2** decomposed through two endothermic stages maximized at 142 and 425 ^{o}C corresponding to desorption of 1.5 hydrated water molecule (observed mass loss 4.16, calcd. 4.73%) two coordinated water and Tp, respectively, with overall mass loss amounting to 84.96% (calcd. 89.71%) leaving Ni/NiO as a final residue, the TGA/DTA curves of complex **3** exhibit only one decomposition step at 350 ^{o}C assigned to exclusion of one H-bonded ethanol and two Tp molecules with overall mass loss amounting to 89.99% (calcd. 89.30%) leaving copper metal as a final residue at 600 ^{o}C. Thermal degradation of complex **4** proceeds *via* three main steps at 100, 377, and 450 ^{o}C assigned to loss of H_2O hydrated molecule and 2 Tp molecules leaving Zn metal as residue with overall mass loss amounts to 89.23% (calcd. 87.70%).

3.4. Electronic structure and magnetic susceptibility

The electronic spectrum of Tp displayed four absorption bands in ethanol at 210, 239, 297 and 337 nm (Figure 2). The bands at 210 and 239 nm may be assigned to the medium and low energy π-π^* transitions within the phenyl rings, respectively [26]. The band at 297 nm is attributed to the π-π^* transition within the triazole ring. The geometry of T_p suggests the formation of an intra-molecular H-bond, which will force the lone pair of the OH group to be parallel with the π cloud, and thereby, increases the resonance character of this group with the triazoles moiety [27]. This resulted in the appearance of a band at 337 nm. The electronic spectrum of Tp was recorded in solvents of different polarities and H-bond formation tendencies, such as 2-propanol, acetonitrile, cyclohexane, chloroform, ethanol, and dioxane (Figure 2). The band at 205 nm in acetonitrile is slightly red-shifted in ethanol and 2-propanol (H-bonding solvents) suggesting that Tp is acting as a proton acceptor [28] at the triazole-type nitrogen.

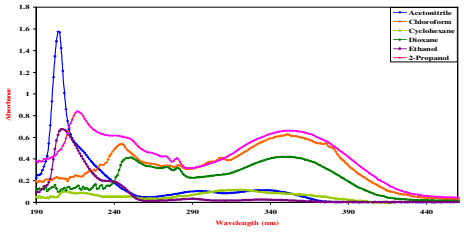

Figure 2: Electronic absorption spectra of Tp in different solvents

The electronic spectra of 10^{-4} M of the complexes were reported in DMF, Figure 3. The bands observed at 262, 292, and 339 nm may be assigned to the internal ligand transitions.The d-d transitions of the complexes were very weak to be observed at this concentration, so, the absorption of the solid complexes was measured (Figure 3 the inset).Complex **1** showed a band at 770 nm that may have accounted for the $^4T_{1g}(F)\rightarrow{}^4A_{2g}$ transition in an octahedral geometry. The solid-state absorption spectrum of **1** supports the solution spectrum by observing another band in the visible region at 576 nm assigned to the $^4T_{1g}(F)\rightarrow{}^4T_{1g}(P)$ transition. (inset Figure 3) The μ_{eff} of 4.29 μ_B for complex **1** further complements the electronic spectral findings. This value is in the acceptable experimental range (4.10-5.20 μ_B) for high spin Co(II) complexes [29]. The electronic spectrum of complex **2** showed two additional bands around 538 and 637 nm assigned to $^3A_{2g}$ (F) $\rightarrow$ $^3T_{1g}$ (P), $^3A_{2g}$ (F) $\rightarrow$ $^3T_{1g}$(F),transitions, which is characteristic of octahedral geometry [30]. The magnetic moment of complex **2** is found to be 4.63 μ_B, which may be taken as a criterion for the presence of tetrahedral or square-pyramidal stereochemistry [31]. Complex **3** showed a band centered at 840 nm, which can be assigned in terms of overlapping the ν_1-ν_3 bands in a distorted octahedral geometry [32]. The reflectance spectrum exhibited a band at 582 nm allocated for $^2B_{1g}\rightarrow{}^2B_{2g}$ transition. The μ_{eff} value of **3**, corrected for diamagnetic and temperature-independent paramagnetic contributions, was found to be 2.13 μ_B (298 K). This indicates the presence of monomeric species without any interaction between the Cu(II) ions from the neighbouring molecules. Tetrahedral stereochemistry [33] was suggested for the diamagnetic Zn(II) complex **4** based on elemental analyses and TGA.

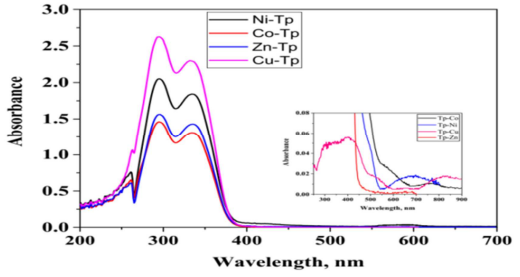

Figure 3: Absorption spectra of Tp complexes (inset represent absorption of Tp and

3.5. EPR study

The X-band EPR spectrum of complex **3** in solid state (Figure 4) at 298 K shows $g_{\parallel}$ = 2.278 and $g_{\perp}$ = 2.120 characterized of mononuclear copper (II) complex having rhombic-octahedral with the elongation of the axial bonds and $d_{x^2-y^2}$ orbital is the ground state. The geometric parameter G, which is a measure of the exchange of interaction between the copper centers in a powdered sample, has been calculated [34] as$G = (g_{\parallel} - 2.0023)/(g_{\perp} - 2.0023)$. According to Hathaway [35] if G > 4, the exchange interaction is negligible and if G < 4, indicates exchange interaction. The value of G is found to be 2.25indicating the presence of moderate exchange interaction among the copper molecules in the solid state.

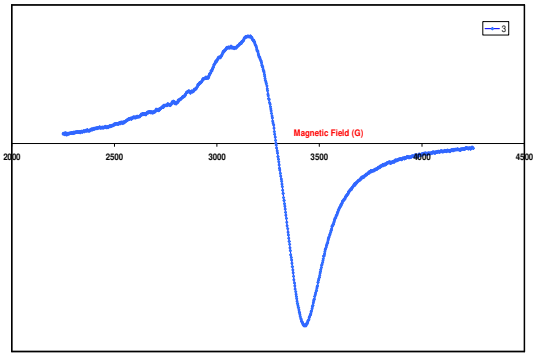

Figure 4: EPR spectrum of complex 3

From the previous analysis, it can be concluded that a tetrahedral structure has been proposed for the Zn–Tinuvin-P (TP) complex, on the other hand, nickel (II), cobalt(II), and Copper (II) forms with Tinuvin-(TP) complexes in agreement with an octahedral environment around the metal ion as shown in Scheme 1 below.

3.6. XRD study

The XRD patterns of complexes 1-4 are presented in Figure 5. It is obvious from this figure that complex 1 is amorphous while complexes 2-4 are semicrystalline.

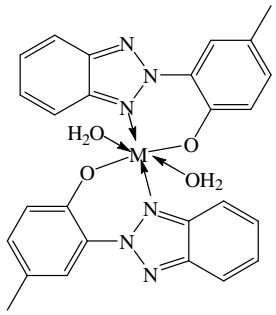

M = Co (**1**), Ni (**2**) and Cu (**3**)

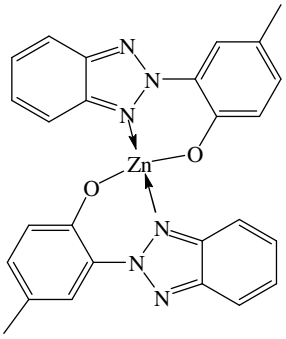

(**4**)

Scheme 1

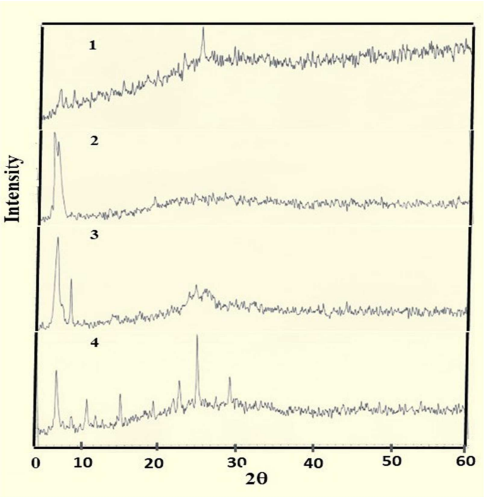

Figure 5. XRD patterns of complexes 1-4

3.7. Photo stabilization of PVC

The efficacy of the investigated stabilizers in photo-stabilization has been evaluated based on two criteria, namely weight loss and gel formation. It is

widely known that the photodegradation of PVC is associated with the dehydrochlorination process, leading to the release of HCl gas and subsequent weight loss, which is exacerbated with prolonged irradiation time. Thus, the weight loss percentage as a function of the irradiation time could be considered as a convenient means for the determination of the degree of photodegradation and consequently can measure the stabilizing effectiveness of the stabilizer, and how long the stabilizer protects the polymer. The results of the weight loss % of the different investigated Tp-complex stabilizers taken in 2 wt% based on PVC weight as a function of the photo-degradation time are tabulated in (Table 1). The results of the blank sample and the sample stabilized with the parent Tp as a reference stabilizer are also given for comparison.

The results clearly reveal the low extent of weight loss (i.e., low extent of dehydrochlorination) of photo-degraded PVC stabilized with the investigated Tp-complexes as compared with the blank sample and the low extent of weight loss % of Tp-Co (**1**) and Tp-Ni (**2**) complexes as compared with the unmodified reference UV-stabilizer (Tp), while Tp-Cu (**3**) and Tp-Zn (**4**) complexes gave a slightly higher weight loss % as compared with the reference Tp.On the other hand, the best-stabilizing efficiency of the investigated complexes is given by the Co-complex (1), as after 8h irradiation, its weight loss is only 40.7% that of the blank and 56.44% that of the reference stabilizer (Figure 6). This behavior can be interpreted in terms of the electronic configuration of the metal center, type of coordinating anion, and stability rather than geometry, and metal-to-ligand ratio. For example, complexes **1** and **3** have the same stereochemistry and coordinating anion, but the metal central atom are different**.**

Preliminary studies on photo-degraded PVC blank and photodegraded PVC stabilized with the investigated Tp-complexes have proven the formation of gels. For this, the extent to which gels are formed can be taken as a measure of the efficiency of stabilization. The obtained results of the % gelation of photodegraded PVC blank and for PVC stabilized with either of the investigated Tp-complexes stabilizers together with the blank PVC sample and the sample stabilized with Tp reference stabilizer after 8h irradiation are represented in (Table 1). The results reveal that the extent of gelation follows the ascending order: *Tp-Ni ˂Tp-Zn ˂Tp-Co ˂Tp˂Tp-Cu ˂ Blank PVC*. Moreover, the data obtained for the % soluble fractions for the various PVC films stabilized with the aforementioned Tp-complexes together with the data of the blank PVC and that stabilized with the reference Tp after 8h irradiation time agree well with the data obtained for the % gelation, which gives an additional proof for the amount of gel formation.

Table (1): Weight loss (%), soluble fraction (%), and gel content (%) measurements for rigid PVC in the presence of Tp complexes acting as photostabilizers compared to Tpas a reference stabilizer

Material	Weight loss (%)	Gel content (%)	Soluble fraction (%)
PVC (2 h)	13.68	12	86
PVC (4 h)	17.46	17	82
PVC (6 h)	19.62	21	79.50
PVC (8 h)	20.63	25.84	74.07
PVC +Tp (Ref.) (2 h)	4.45	16	83
PVC +Tp (Ref.) (4 h)	6.85	23.50	76
PVC +Tp (Ref.) (6 h)	8.91	25	74
PVC +Tp (Ref.) (8 h)	14.90	16.44	83.25
PV + (Co(II) -Tp) (2 h)	0.86	2	97.50
PVC + (Co(II) -Tp) (4 h)	2.31	18.50	81
PVC + (Co(II) -Tp) (6 h)	5.79	23	76
PVC + (Co(II) -Tp) (8 h)	8.41	11.14	88.70
PVC + (Ni(II) -Tp) (2 h)	0.84	1.4	98
PVC + (Ni(II) -Tp) (4 h)	3.20	10	89.50
PVC + (Ni(II) -Tp) (6 h)	6.22	26	73
PVC + (Ni(II) -Tp) (8 h)	10.71	15.90	84. 10
PVC + (Cu(II) -Tp) (2 h)	8.45	21.5	78
PVC + (Cu(II) -Tp) (4 h)	8.80	23	76.50
PVC + (Cu(II) -Tp) (6 h)	9.59	25	74
PVC + (Cu(II) -Tp) (8 h)	15.23	21.80	78.13
PVC + (Zn(II) -Tp) (2 h)	7.60	14	85
PVC + (Zn(II) -Tp) (4 h)	8.03	21	78
PVC + (Zn(II) -Tp) (6 h)	10.52	16.50	83
PVC + (Zn(II) -Tp) (8 h)	16.27	12.23	87.56

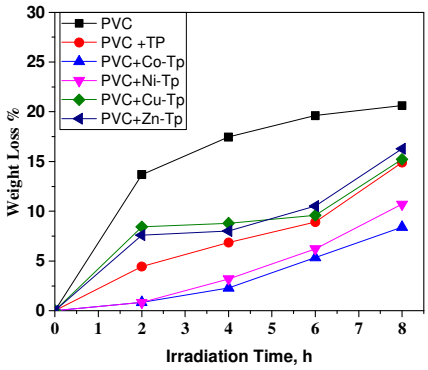

Figure 6: Variation of weight loss (%) of M(II)-Tp complexes with time of irradiation (h)

3.8. SEM analysis of the polymer surface

The surfaces of the PVC with pure Tp and three Tp-complexes before and after irradiation were further investigated using SEM. SEM images offer undistorted and visually distinct surface representations, enabling the observation of particle homogeneity as well as accurate measurement of particle size and shape. Alotaibi et al. found that the SEM images of the PVC film before irradiation were generally smooth and after irradiation showed damage within the PVC surface and the formation of many cracks because of photodegradation of polymeric chain with white spots, groves, and lumps indicating a high level of photodegradation [36]. The non-irradiated pure Tp-PVC film displayed a uniform and sleek surface. However, upon irradiation, numerous pores emerged on the PVC surface, signifying the occurrence of photodegradation in the PVC film, as depicted in Figure 7.

The morphology of the PVC sample doped with cobalt and nickel complexes has changed to a hexagonal shape. The PVC stability can be significantly enhanced by the hexagonal shape of the Ni(II) or Co(II) ions, which serve as short-term stabilizers. Also, the SEM study showed that the synthesized PVC film containing Ni complex was highly honeycomb-like structure after 4hs of irradiation. Previous studies reported the existence of a honeycomb-like structure in PVC blended with a Schiff base that includes a dithiazole moiety and nickel chloride [37,38]. The hexagonal honeycomb structure could be formed due to the interaction and/or coordination between the PVC-Schiff base blend and Ni (II) ion as a result of cross-linking. The same honeycomb-like structure could be seen for the irradiated PVC films containing cobalt complexes. Previous reports suggested that cross-linked materials are ideal for producing honeycomb-like structures [37]. It is believed that honeycomb structure is significantly influenced by several factors, including the type of solvent, the length of polymer sidechains, and the concentration of the polymer [39, 40]. However, in the present case, it seems that the structure depends on the metal used in the complexation and the complex structure. The SEM image of the Cu-complex exhibited a porous structure but not a honeycomb structure. The reason for these phenomena remains uncertain; however, they may be attributed to a sluggish HCl elimination rate and its subsequent entrapment by the metal complex.

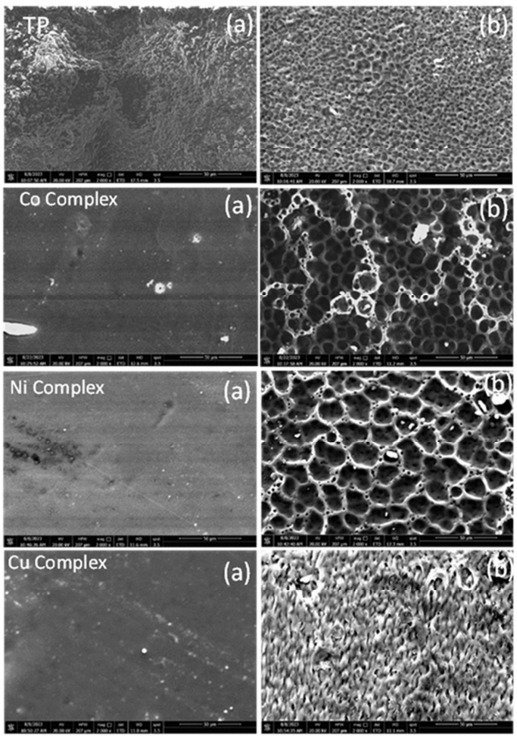

Figure 7: SEM of PVC with pure Tp and Tp-complexes (a) before and (b) after irradiation

The photodegradation process of PVC leads to the dehydrochlorination in which hydrogen chloride gas evolved with PVC weight loss and the formation of cross-linked chains which could be the reason for the honeycomb porous structure formation.

Different suggestions have been proposed for the function of metal complexes [41]. One such suggestion is that metal complexes can form coordinated bonds with PVC chains through polarized bonds, resulting in the stabilization of polymeric materials (Scheme 2a). The presence of aromatic groups in these complexes enhances the stability of the excited state intermediate, thereby minimizing PVC damage [42]. Additionally, the metal atom can serve as a secondary stabilizer for PVC. It acts as an HCl scavenger, effectively reducing the detrimental impact on the polymeric chains (Scheme 2b).

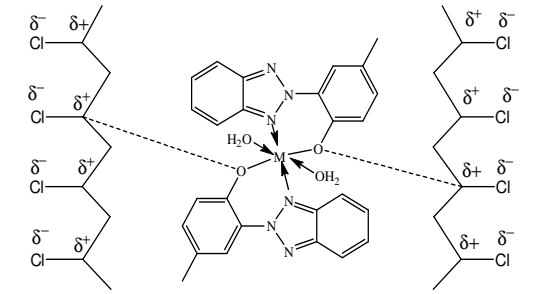

(a)

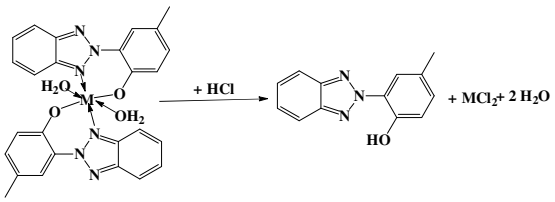

(b)

Scheme 2

3.9. Molecular DFT calculation

To Shed further light on the efficiency of Tp and its complexes, as well as their electronic structures, we conducted an optimization of the ligand and its investigated complexes. This optimization aimed to determine the lowest energy configurations using the Gaussian 09 software at the B3LYP/6-311G (d, p) level, based on the density functional theory (DFT) approach, Figure 8.

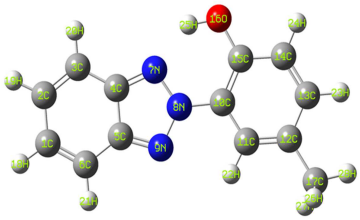

$C_{13}H_{11}N_3O$

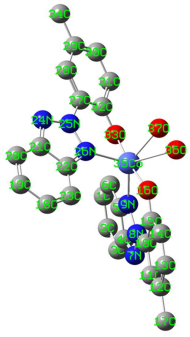

$C_{26}H_{24}N6CoO_4$

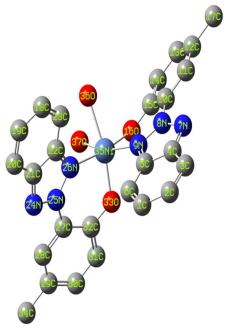

$C_{26}H_{24}N_6NiO_4$

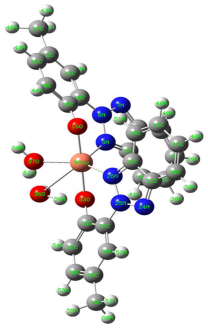

$C_{26}H_{24}N6CuO_4$

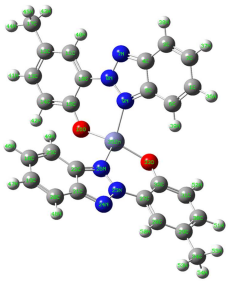

$C_{26}H_{20}N_6O_2Zn$

Figure 8: The numbering system, the optimized structure, net charge, and the vector of the dipole moment of [$C_{13}H_{11}N_3O$ (L), $C_{26}H_{24}N_6NiO_4$, $C_{26}H_{24}N6CoO_4$, $C_{26}H_{24}N6CuO_4$, and $C_{26}H_{20}N_6O_2Zn$. by density function B3LYP/6-311++g(d, p)

The dipole moment (μ), ionization potential (I), electron affinity (A), electronegativity (χ), chemical potential (μ), hardness (H), softness (S), and electrophilicity index (ω) are important quantum chemical descriptors that can be utilized to analyze the ligand (L) and its complexes. These descriptors provide valuable insights into various aspects of reactivity associated with chemical processes and can

be calculated using frontier molecular orbitals, namely the highest occupied molecular orbital (HOMO) and lowest unoccupied molecular orbital (LUMO) energies. Figure 9 illustrates the HOMO and LUMO contours, while Table 2 presents the calculated values for these descriptors.

The frontier molecular orbital (FMO) energy parameters, including E_{HOMO}, E_{LUMO}, and Eg (E_{LUMO}-E_{HOMO}), are commonly utilized to assess the reactivity and stability of structures. The complexes exhibit greater stability compared to the free ligands, as indicated by their more negative total energy. This stability is attributed to the chelation of the ligand to metal ions, resulting in a lower energy gap (Eg) for the complexes, as demonstrated in Table 2. The order of Eg (eV), which indicates the compound's stability, is as follows: Co(II) < Zn (II) < Ni(II) < Cu(II) < Tp. A molecule with a higher Eg possesses lower chemical reactivity but higher kinetic stability. Therefore, the Co(II) complex with an Eg of 2.94 eV is the most reactive complex.

Moreover, it is widely recognized that the HOMO orbital is directly linked to the ionization potential (electron donation), while the LUMO orbital is directly linked to the electron affinity [43]. A molecule with a higher EHOMO value is more likely to donate its loosely bound electrons to the appropriate orbitals of an acceptor molecule. Based on the decreasing order of EHOMO of the current compounds (Table 2), Co(II) > Ni(II) > Cu(II) > Zn(II) >Tp, it can be inferred that the Co(II) complex has the greatest tendency to donate its most energetic electrons to a suitable orbital of an acceptor molecule.

Table 2: Calculated energies and properties of L($C_{13}H_{11}N_3O$), $C_{26}H_{24}N_6NiO_4$, $C_{26}H_{24}N6CoO_4$, $C_{26}H_{24}N6CuO4$ and $C_{26}H_{20}N_6O_2Zn$

Parameter	$C_{13}H_{11}N_3O$	$C_{26}H_{24}N_6NiO_4$	$C_{26}H_{24}N6CoO_4$	$C_{26}H_{24}N6CuO_4$	$C_{26}H_{20}N_6O_2Zn$
Total energy (a.u.)	-741.251	-1779.553	-1803.755	-1803.578	-1547.18
HOMO (eV)	-5.86	-5.38	-5.16	-5.52	-5.54
LUMO (eV)	-2.09	-2.27	-2.22	-2.21	-2.46
E_g (eV) = $E_{LUMO} - E_{HOMO}$	3.77	3.11	2.94	3.30	3.07
Dipole moment Debye	2.2156	1.6066	3.778	1.5167	3.42
Ionization potential I (eV) $-E_{HOMO}$	5.86	5.38	5.16	5.52	5.54
Electron Affinity A (eV) $-E_{LUMO}$	2.09	2.27	2.22	2.21	2.46
Electronegativity χ(eV) = ½ (I + A)	3.98	3.83	3.69	3.86	4.00
Hardness η (eV) = = ½ (I – A)	1.89	1.56	1.47	1.65	1.54
Softness S(eV) = = ½ η	0.94	0.78	0.74	0.83	0.77
ChemicalPotential = -χ	-3.98	-3.83	-3.69	-3.86	-4.00
Electrophilicity power ω (eV) =	4.19	4.70	4.62	4.52	5.21

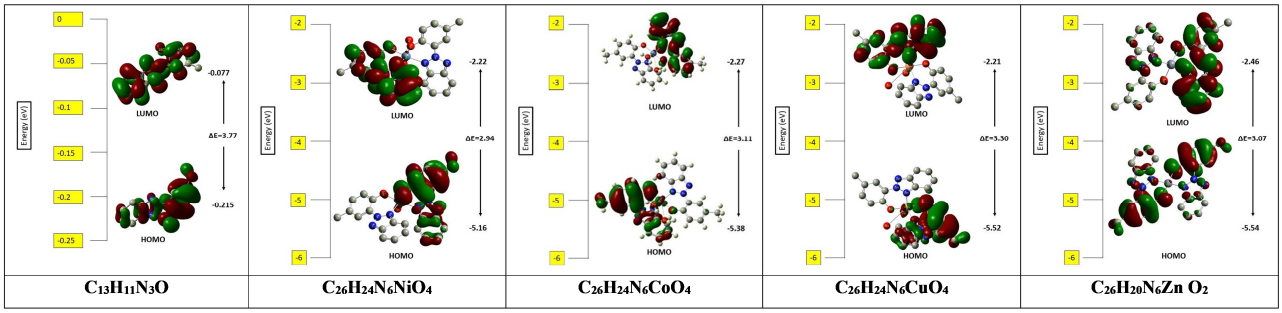

Figure 9: The atomic orbital compositions of the frontier molecular orbital of L($C_{13}H_{11}N_3O$), $C_{26}H_{24}N_6NiO_4$, $C_{26}H_{24}N6CoO_4$, $C_{26}H_{24}N6CuO_4$ and $C_{26}H_{20}N_6O_2Zn$

In contrast, the E_{LUMO} values presented in (Table 2) indicated a specific order for the studied complexes: L >Cu(II) > Co(II) > Ni(II) > Zn(II)-complex. This order suggests that the Zn(II) complex exhibits the greatest tendency to receive electrons from the suitably occupied orbitals of an electron-donating species [44]. The reactivity of the current compounds against photodegradation (weight loss) nearly agrees with the increasing of the calculated chemical potential, Co(II) >> Ni> Cu >Tp> Zn (Table 2) as the relation between weight loss and chemical potential is found to fit straight line with correlation coefficient (R^2 = 0.81). Therefore, the Co (II)-complex, which has the lower ionization potential, higher dipole moment, and lowest E_g, was found to be more highly reactive as a light stabilizer agent than the ligand and other complexes.

4. Conclusion

Novel Co^{II}, Ni^{II}, Cu^{II}, and Zn^{II} complexes were synthesized, characterized, and tested as light stabilizer agents. Based on the results of elemental analyses, spectral, thermal, and conductance values, distorted octahedral geometry is suggested for the complexes $[Co(Tp)_2(H_2O)_2].0.5EtOH$ (1), $[Ni(Tp)_2(H_2O_2)].1.5H_2O$ (2) and $[Cu(Tp)_2(H_2O)_2].EtOH$ (3) while tetrahedral stereochemistry was suggested for the $[Zn(Tp)_2].H_2O$ (4). Structural studies of Co^{II}, Ni^{II}, Cu^{II}, and Zn^{II} complexes of Tinuvin-P, a common industrial PVC UV-stabilizer, have been performed both experimentally and theoretically. Investigation of the studied compounds as photo-stabilizers for PVC composites has been also explored. The results revealed the low extent of weight loss, gelation formation, and development of the soluble fraction of the photo-degraded PVC stabilized by metal complexes comparedto the parent UV absorber. The stabilizing efficiency of the investigated compounds was found to be in the following order:

Co-Tp> Ni-Tp>Tp> Zn-Tp ~ Cu-Tp.

This order can be interpreted in terms of the electronic configuration of the metal center, type of coordinating anion, stability of complex rather than geometry, and metal-to-ligand ratio.

5. References:

[1] Wypych, G., (2020). PVC Formulary, 3rd edition, Toronto, ChemTec Publishing.

[2] Yousif, E., Hameed, A., Rasheed, R., Mansoor, H., Farina, Y., Graisa, A., Salih, N., Salimon, J. (2010). Synthesis and photostability study of some modified poly(vinyl chloride) containing pendant benzothiazole and benzimidazole ring. Int. J. Chem., 2, 65-80.

[3] Turner, A., Filella, M. (2021). Polyvinyl chloride in consumer and environmental plastics, with a particular focus on metal-based additives. Environ. Sci. Process. Impacts, 23, 1376-1384.

[4]Gardette, J., Gaumet, S., Philippart, J.L. (1993). Influence of the experimental conditions on the photooxidation of poly(vinyl chloride). J. Appl. Polym. Sci., 48, 1885-1895.

[5] Mahdi, S. A., Ahmed, A. A., Yousif, E., Al-Mashhadani, M. H., Ahmed, Hashim, A. H.,Jawad, A. H. (2022). New organic PVC photo-stabilizers derived from synthesized novel coumarine moieties, Materials Science for Energy Technologies, 5, 278-29.

[6] El-Hiti, G., Hayal, M., Ahmed, A., Hamad, B., Ahmed, D.S., Ahmed, A., Hashim , H., Yousif, E. (2019). The Morphology and Performance of Poly(Vinyl Chloride) Containing Melamine Schiff Bases against Ultraviolet Light, Molecules, 24, 803, 1-15.

[7] Ali, M., El-Hiti, G., Yousif, E. (2016). Photostabilizing Efficiency of Poly(vinyl chloride) in the Presence of Organotin(IV) Complexes as Photostabilizers, molecules, 21(1151), 1-16.

[8] Haddad, R., Yousif, E., Yusop, R. M. (2014). Ultra violet spectra studies of polystyrene films in presence of some transition metal complexes with 4-amino-5-pyridyl)-4h-1,2,4-triazole-3-thiol. Orient J Chem; 30(4), 1565-1569.

[9] Crawford, J.C. (1999). 2(2-hydroxyphenyl)2H-benzotriazole ultraviolet stabilizers. Prog Polym Sci., 24(1),7-43.

[10] Chanda, M., Roy, S.K. (2010). Plastic Technology Handbook, 4th ed., Plastic Engineering Series CRC,

[11] Poveda, P. N. S. and Silva, L.G.A. (2017). Characterization of Minerals, Metals and Materials, Springer International Publishing.

[12] Fahem R., Yousif (2017) Photo-Irradiation of Polymer Films: Review. J. Thin Films Res. 1 ,17–23.

[13] Cui Z., Li X., Wang X., Pei K., Chen W. (2013),Structure and properties of N-heterocycle-containing benzotriazoles as UV absorbers,Journal of Molecular Structure,1054–1055,94-99.

[14] El-Asmy, H.A., Butler, I.S., Mouhri, Z.S., Jean-Claude, B.J., Emmam, M.S., Mostafa, S.I., J. (2014). Zinc(II), ruthenium(II), rhodium(III), palladium(II), silver(I), platinum(II) and complexes of 2-(2′-hydroxy-5′-methylphenyl)-benzotriazole as simple or primary ligand and 2,2′-bipyridyl, 9,10-phenanthroline or triphenylphosphine as secondary ligands: Structure and anticancer activity, Mol. Struct., 1059, 193-201.

[15] Carofiglio, T., Solari, E., Flo*riani,* C. (1996). UV stabilizers bonded to transition metals: Synthesis and X-ray structure of 2-(2′-hydroxyphenyl)benzotriazole-oxovanadium(IV) and -dioxomolybdenum(VI) complexes. Polyhedron, 15(24), 4435-4440.

[16] E. Yousif, A. Hasan, G.A. El-Hiti. (2016). Spectroscopic, physical and topography of photochemical process of PVC films in the presence of Schiff base metal complexes, Polymers, 8 204
[17] Weinhold, F. (2012).Natural bond orbital analysis: a critical overview of relationships to alternative bonding perspectives, J ComputChem.. 33, 2363-79.
[18] Mansour, A.M. (2014). Synthesis, spectroscopic, electrochemical, DFT and SAR studies of nifuroxazide complexes with Pd(II), Pt(II) and Ru(II). Polyhedron, 78, 10-17.
[19] Abdel-Ghani, N.T., Abo El-Ghar, M.F., Mansour, A.M. (2013). Novel Ni(II) and Zn(II) complexes coordinated by 2-arylaminomethyl-1H-benzimidazole: Molecular structures, spectral, DFT studies and evaluation of biological activity. Spectrochim. Acta A 104, 134-142.
[20] Frisch, M.J., Trucks, G.W., Schlegel, H.B., Scuderia, G.E., Robb, M.A., Cheeseman, J.R., Scalmani, G., Barone, V., Mennucci, B., Petersson, G.A., et al. (2009). Gaussian 09, Revision a. 02, Gaussian Inc, Wallingford, CT, USA.
[21] Margulis, L.A., Gorelik , B.A., Semenenko, E.I. (1983). Effect of tetrahydrofuran on radiation-induced and thermal oxidation of polyvinyl chloride. Polymer science U.S.S.R,Volume 25, Issue 3, 775-777.
[22] Sabaa, M.W., Oraby, E.H., Abdel-Naby, A.S., Mohamed, R.R.(2005). Anthraquinone derivatives as organic stabilizers for rigid poly(vinyl chloride) against photo-degardation. Eur. Polym. J. 41, 2530-2543.
[23] El-Sayed, S., Jean, B. (2012). Synthesis, structural characterization and anticancer activity of some new complexes of 6-amino-4-hydroxy-2-thiopyrimidine. J. Mol. Struct. 1028, 208-214.
[24] Loukopoulos E., Kostakis G. E. (2019) Recent advances in the coordination chemistry of benzotriazole-based ligands, Coordination Chemistry Reviews, 395, 193-229.
[25] Claramunt, R. M., María, D. S., Pinilla, E., Torres, M R , Elguero, J. (2007). Structural studies of two Tinuvin P analogs: 2-(2,4-dimethylphenyl)-2H-benzotriazole and 2-phenyl-2H-benzotriazole, Molecules.12(9), 2201-14.
[26] Santa María D., Claramunt R. M., Bobosik V., Torralba M. C., Torres M. R., Alkorta I., Elguero J. (2013) Synthesis and structural study of 2-arylbenzotriazoles related to Tinuvins, Tetrahedron, 69, 3027-3038.
[27] Pike, S. J., Hunter, C. A. (2017). Fluorescent and colorimetric molecular recognition probe for hydrogen bond acceptors, 15(45), 9603-9610.
[28] Görner, H. (2001). Photochromism of nitrospiropyrans: effects of structure, solvent and temperature. Phys. Chem. Chem. Phys., 3, 416-423.
[29] Mondala, N., Deya, D.K., Mitra, S., Abdul Malik, K.M. (2000). Synthesis and structural characterization of mixed ligand η^1-2-hydroxyacetophenone complexes of cobalt(III). Polyhedron 19, 2707-2711.
[30] González, Emmanuel, Rodrigue-Witchel, Alexandre, Reber, Christian. (2007). Absorption spectroscopy of octahedral nickel(II) complexes: A case study of interactions between multiple electronic excited states, Coordination Chemistry Reviews, 251, 351-363,
[31] Carballo, R., Castineiras, A., Hiller, W., Strahle, J. (1993). Nickel(II) complexes of 1,7-bis(benzimidazol-2-yl)-2,6-dithiaheptane (BBDHP). Crystal and molecular structure of $[Ni_2(BBDHP)_2(\mu\text{-}Cl)_2]Cl_2\cdot 5H_2O\cdot 2EtOH$ and $Ni(BBDHP)Br_2\cdot EtOH.Bu^tOH$. Polyhedron, 12, 1083-1092.
[32] Ruiz, R., Lloret, F., Julve, M., Faus, J., Munoz, Mc and Solans, X. (1993).A study of the exchange interaction through phenolato, oximato and oxamidato bridges in $Mn^{II}Cu^{II}$ dimers. Crystal structure of $[Cu(salen)Mn(hfa)_2]$. Inorg. Chim. Acta, 213, 261-268.
[33] Rehman, S.U., Ikram, M., Rehman, S. (2010). Synthesis and biological studies of complexes of 2- amino-N(2-aminobenzoyl) benzohydrazide with Co(II), Ni(II), and Cu(II).*Frontiers of Chemistry in China*5, 348-356.
[34] Pantcheva, I.; Stambolivska, R.; Petkov, N.; Tadier, A.; Simova, S.; Stoyanova, R.; Kukeva, R.; Dorkov, P. (2022) Dinuclear vs. Mononuclear Copper(II) Coordination Species of Tylosin and Tilmicosin in Non-Aqueous Solutions. *Molecules* , *27*, 3899.
[35] Dudley, R.J., Hathaway, B.J. (1970). Single-crystal electronic and e.s.r. spectra of bis-(aquo)monoacetylacetonatocopper(II) picrate, J. Chem. Soc., 1725-1728.
[36] Alotaibi, M.H.; El-Hiti, G.A.; Hashim, H.; Hameed, A.S.; Ahmed, D.S.; Yousif, E. (2018). SEM analysis of the tunable honeycomb structure of irradiated poly (vinyl chloride) films doped with polyphosphate. Heliyon, 4, e01013.
[37] Hashim, H., A. El-Hit,i G., Alotaibi, M.H., Ahmed, D. S., Yousif, E. (2018). Fabrication of ordered honeycomb porous poly(vinyl chloride) thin film doped with a Schiff base and nickel(II) chloride. Heliyon, 4, e00743.
[38] Jasem, H.; Hadi, A.G.; El-Hiti, G.A.; Baashen, M.A.; Hashim, H.; Ahmed, A.A.; Ahmed, D.S.; Yousif, E. (2021). Tin-naphthalene sulfonic acid complexes as photostabilizers for poly(vinyl chloride). Molecules, 26, 3629.
[39] Liu, C., Lang, W., Shi, ,B., Guo, Y. (2013). Fabrication of ordered honeycomb porous polyvinyl chloride (PVC) films by breath figures method. Materials Letters, 107, 53-55.
[40] Huh, M. , Gauthier, M., Yun, S.I., (2016). Honeycomb structured porous films prepared from arborescent graft polystyrenes via the breath figures method Polymer,107, 273-281.
[41] Mohammed, A.; El-Hiti, G.A.; Yousif, E.; Ahmed, A.A.; Ahmed, D.S.; Alotaibi, M.H.

(2020). Protection of poly(vinyl vhloride) films against photodegradation using various valsartan tin complexes. Polymers, 12, 969.

[42] Sabaa, M.W.; Oraby, E.H.; Abdul Naby, A.S.; Mohamed, R.R. (2005). N-Phenyl-3-substituted-5-pyrazolonederivatives as organic stabilizer for rigid PVC against photodegradation. J. Appl. Polym. Sci., 101, 1543-1555.

[43] Mohamed, S. E, Ramadan, R. M, , Aboelhasan, A. E, , Abdel Aziz, A. A. (2023). Design, synthesis, biomedical investigation, DFT calculation and molecular docking of novel Ru(II)-mixed ligand complexes. J. Biomol. Struct. Dynan., 41, 1233-1252.

[44] Abdel Aziz, A. A, Ramadan, R. M., Sidqi, M. E., M. Sayed, A. (2023). Structural characterisation of novel mononuclear Schiff base metal complexes, DFT calculations, molecular docking studies, free radical scavenging, DNA binding evaluation, and cytotoxic activity, Appl.Organomet. Chem. 37(2), e6954.